Supplemental Methods

Mice

To generate mice with a floxed allele of the NADPH oxidase subunit *Ncf2* (*Ncf2*$^{fl/fl}$ mice), we bred B6.129S4-Gt(ROSA)26Sor$^{tm1(FLP1)Dym}$/JRainJ mice[1] (JAX stock 009086) with homozygous Ncf2$^{tmla(EUCOMM)Wsti}$ C57BL/6 mice produced as described.[2] The Ncf2$^{tmla(EUCOMM)Wsti}$ allele harbors a conditional-ready insertion and loxP sites that can delete exon 3 of Ncf2 to generate a frameshifted transcript and null allele. *Ncf2*$^{fl/fl}$ mice were crossed to B6.129P2-Lyzs$^{tm1(cre)Ifo}$/J mice[3] (JAX stock 004781), commonly known as LysMCre mice, to generate *Ncf2*$^{fl/fl}$ LysM$^{WT/Cre}$ offspring, referred to as *Ncf2*^{LysMCre} mice

To generate germfree mice, *Cybb*^{KO} mice were maintained as homozygous breeding colonies and re-derived germfree (GF) at the University of Louisville's Gnotobiotic Mouse Facility (UoLGMF). Briefly, Swiss Webster mice and *Cybb*^{KO} mice were time-mated. Just prior to delivery of the pups, pregnant females were euthanized and the uterus collected en-bloc. Pups were removed aseptically and cross-fostered by SW females that had age matched litters. The *Cybb*^{KO} GF breeding colony was maintained in a flexible film isolator on soft bedding, and fed autoclaved rodent chow (Envigo Tekland 2019S) ad libitum and provided autoclaved water. Age and sex matched control GF C57BL/6 (originally obtained from Taconic) mice were obtained from the UoLGMF breeding colonies. GF status of individual animals in the GMF core is determined routinely two to three times per month by 16s rRNA PCR profiling of feces for bacterial and fungal species and in routine testing of isolaters themselves by fungal cultures. Sentinels in the facility are also monitored for viruses and other pathogens per Specific Pathogen Free protocols.

Isolation of cells from bronchoalveolar lavage and lung

Bronchoalveolar lavage (BAL) cells was harvested through the trachea by 3 sequential 1 ml lavages with ice cold PBS (Sigma)+1%FBS (Atlanta Biologicals) + 2mM EDTA (Corning) and analyzed for cell counts, differential by Wright-Giemsa cytospins (Hema 3^{TM}, Fischer) and/ or flow cytometry, and cytokine levels by ELISA as described.[4] In some experiments, the right inferior lobe of lung was harvested, minced and submerged in digestion buffer containing collagenase D (5mg/ml) and DNase (1mg/ml) and incubated at 37 ºC for 40 min with constant shaking, then strained and single cells isolated as described.[4] RBC lysis were performed using ACK lysis buffer (Gibco).

Flow cytometry analysis and sorting

BAL and isolated single cells from lungs were washed with flow buffer (PBS, 2%FBS and 2mM of EDTA) and counted. Samples incubated with anti-mouse CD16/32 (clone 2.4G2, BioXcell) to block Fc-receptors. Equal number of cells were then stained in the dark with various antibodies (Table 1) for 30 mins at 4°C. Alveolar macrophages were identified as $CD45^+$Siglec F^+ $CD11c^+$, neutrophils as $CD45^+$Siglec F^- $Ly6G^+$ and eosinophils as $CD45^+$Siglec F^+ $CD11c^-$. Samples were washed and flow cytometry was performed. Data was collected on a Cytek modified FACScan (BD Biosciences and Cytek Development). Flow jo (v10.1) was used to analyze the data. The gating strategy is shown in Supplemental Figure 1.

For sorting, BAL cells were isolated, washed and counted. Surface receptor staining was performed as mentioned before. Cells were washed with FACS buffer and sorted using a BD FACSAria™ Fusion (BD Biosciences) and the 100um nozzle was used. PMNs were gated out first by Ly6G expression then $CD45^+$Siglec F^+ $CD11c^+$ $CD11b^{high}$ cells were sorted from $CD45^+$Siglec F^+ $CD11c^+$ $CD11b^{low}$cells. Cells were collected into RPMI (R&D Systems)+20%FBS centrifuged at 400g for 5 mins and processed for RNA isolation using a RNeasy plus kit (Qiagen) following manufacturer's instruction. 96-99% pure populations were obtained.

Preparation and analysis of lung cells by mass cytometry

For analysis of mouse lung cells by mass cytometry, the right lung was minced, digested and single cells were isolated as mentioned above. Lung cells were suspended in FACS buffer (1% bovine serum albumin in PBS) and counted with a hemocytometer using trypan blue (Sigma, 0.1%) exclusion. Cells were suspended in freezing media (50% fetal bovine serum, 40% RPMI 1640, 10% DMSO) and cryopreserved in liquid nitrogen vapor for analysis. Cell preparation for mass cytometry antibody labeling and CyTOF was done following the protocol from[5] on a CyTOF2/Helios (Fluidigm) mass cytometer in the Andrew M. and Jane M. Bursky Center for Human Immunology and Immunotherapy Programs (CHiiPs). Antibodies used for CyTOF are listed in Table 2.

Manual gating was performed using CytoBank software using standard parameters with the focus primarily on monocyte/macrophage cell lineages. After gating out CD45- , CD3+ , CD19+ , B220+ , NK1.1+ , and Ly6Ghigh cells (Lin-), the cell phenotypes were: alveolar

macrophages, Lin+ /SiglecF^{high}; interstitial macrophages, Lin+ /SiglecF- /CD64+ ; dendritic cells, Lin+ /SiglecF- /CD64- /CD11chigh/MHCII^{high}; inflammatory monocytes Lin+ /SiglecF- /CD64- /CD11C^{low}/MHCII^{low}/Ly6Chigh; and patrolling monocytes, Lin+ /SiglecF- /CD64- /CD11clow/MHCII^{low}/Ly6C- /F4/80+ . Using this gating scheme, some Ly6C+ interstitial macrophages remain that previously have been termed monocyte/macrophages. For the purposes of this study, all CD64+ cells were considered macrophages. Data were analyzed using Cytobank software (Cytobank.org)

ELISA and multiplex cytokine array

A multiplex mouse cytokine array was performed on mouse BAL samples using ProcartaPlex panels from Thermo Fisher Scientific in the Immunomonitoring Laboratory within the Andrew M. and Jane M. Bursky Center for Human Immunology and Immunotherapy Programs (CHiiPs). ELISAs (R and D Systems) were used to measure indicated individual cytokines.

Real Time PCR

Total RNA was isolated from either total BAL cells, which were ~90-99% AM, sorted BAL AM or also from a portion of lung tissue using RNAeasy micro-plus columns (Qiagen). For total BAL, samples were washed prior to addition of lysis buffer. For the preparation of RNA from the lungs, a portion of the lungs were snap-frozen in the -80^{o} C until further use. During RNA isolation, tissues were thawed and lysis buffer (Qiagen) was added to it. It was homogenized, centrifuged at 400rpm for 5 mins and the supernatant were used for RNA isolation. RNA was quantified using Nanodrop. Total RNA was reverse transcribed to cDNA using random hexamers, high-capacity cDNA transcription kit (Applied Biosystems) following manufacturer's instructions. All reagents for RT-PCR were purchased from Life Technologies, Thermo Fisher Scientific. TaqMan gene expression primers (Thermo Fisher Scientific) (Table 3) were used, RT-PCR performed on a AB7500 Fast Real Time PCR system (Applied Biosystem) using TaqMan universal PCR master mix. Glyceraldehyde 3- phosphate dehydrogenase (GAPDH) was used to normalize gene expression. Fold change relative quantification (RQ) was calculated using the $^{\Delta\Delta}$CT method.

Histology and Immunohistochemistry

In some experiments, the left lung was harvested after inflation with 10%formalin and fixed in 10%formalin solution. The tissues were dehydrated gradually using graded ethyl alcohol, embedded in paraffin and 5um thin sections were prepared. Tissue sections were stained with hematoxylin and eosin. Histology was scored under 10X magnification as follows: (0:) No change from wild-type control mice (1) Eosinophilic alveolar macrophages (AM) present; (2) Eosinophilic AM with visible intracellular crystals present; (3) (1, 2) and with extracellular crystals present in alveoli; (4) (1-3) and patchy cellular infiltrate (small foci<3 or area <2um); (5) (1-3) and patchy cellular infiltrate (moderate foci >3 or area >2um); (6) (1-3) and patchy cellular infiltrate (foci >5um); (7) (1-3) and patchy cellular infiltrate (foci involve more than 10% of the lung); (8) (1-3) and cellular infiltrate involving more than 50% of alveoli.

For immunohistochemistry, tissues were de-paraffinized using Safe Clear (Fisher), antigen retrieval performed using unmasking solution (Vector Laboratories) according to the manufacture's protocol, then processed and stained for myeloperoxidase and DAB peroxidase substrate as described.[4] Images were captured by Nanozoomer digital slice scanner (Hamamatsu Photonics) and analyzed by NDP.view2 software (Hamamatsu).

Transmission electron and immunoelectron microscopy

For ultrastructural analyses, BAL macrophage samples were fixed in 2% paraformaldehyde/2.5% glutaraldehyde (Polysciences Inc.,) in 100 mM sodium cacodylate buffer, pH 7.2 for 1 hr at room temperature. Samples were washed in sodium cacodylate buffer at room temperature and post fixed in 1% osmium tetroxide (Polysciences Inc.) for 1 hr. Samples were then rinsed extensively in dH20 prior to en bloc staining with 1% aqueous uranyl acetate (Ted Pella Inc., Redding, CA) for 1 hr. Following several rinses in dH2O, samples were dehydrated in a graded series of ethanol and embedded in Eponate 12 resin (Ted Pella Inc.). Sections of 95 nm were cut with a Leica Ultracut UCT ultramicrotome (Leica Microsystems Inc., Bannockburn, IL), stained with uranyl acetate and lead citrate, and viewed on a JEOL 1200 EX transmission electron microscope (JEOL USA Inc., Peabody, MA) equipped with an AMT 8-megapixel digital camera and AMT Image Capture Engine V602 software (Advanced Microscopy Techniques, Woburn, MA).

For immunolocalization, BAL cells were fixed in 4% paraformaldehyde/0.05% glutaraldehyde (Polysciences Inc., Warrington, PA) in 100mM PIPES/0.5mM $MgCl_2$, pH 7.2 for 1 hr at 4°C. Samples were then embedded in 10% gelatin and infiltrated overnight with 2.3M sucrose/20% polyvinyl pyrrolidone in PIPES/$MgCl_2$ at 4°C. Samples were trimmed, frozen in liquid nitrogen, and sectioned with a Leica Ultracut UCT7 cryo-ultramicrotome (Leica Microsystems Inc., Bannockburn, IL). Ultrathin sections of 50 nm were blocked with 5% FBS/5% NGS for 30 min and subsequently incubated with indicated primary antibodies for 1 hr at room temperature. Following washes in block buffer, sections were incubated by the appropriate colloidal gold conjugated secondary antibodies (Jackson ImmunoResearch Laboratories, Inc., West Grove, PA) for 1 hr. Sections were stained with 0.3% uranyl acetate/2% methyl cellulose and viewed by transmission electron microscope as described above. All labeling experiments were conducted in parallel with controls omitting the primary antibody. These controls were consistently negative at the concentration of colloidal gold conjugated secondary antibodies used in these studies.

Proliferation and cell death assays

Incorporation of bromodeoxyuridine (BrdU) was used to quantify the proliferation of alveolar macrophages in naïve mice following manufacturer's protocol (BrdU-FITC kit; BD Bio-Sciences). 0.1mg of BrdU was given intraperitoneally to each mouse for 3 consecutive days. On the 4^{th} day, mice were sacrificed; BAL and lung tissues were harvested. Flow cytometry analysis was done on dispersed lung cells after staining single cells with anti-mouse FITC-BrdU (BD Pharmingen). AM ($CD45^+$Siglec F^+ $CD11c^+$populations that were either $CD11b^+$or $Cd11b^-$) were gated and $BrdU^+$AM were plotted.[6]

Cell apoptosis was determined using the Annexin V Apoptosis Detection kit (BD Bioscience) following manufacturer's protocol. BAL cells were stained initially with BV510 Rat anti-mouse CD45 (Clone 30F11, BD Horizon, San Jose, CA), PE anti-mouse Siglec F(Clone E-50- 2440, BD Pharmingen), APC anti-mouse CD11b (Clone M1/70 eBioscience) and PE anti-mouse CD11c (HL3, BD Pharmingen). Then, these cells were washed twice with annexin binding buffer and the volume was then adjusted to 100ul per sample. 1ul of FITC-Annexin V (BD Bioscience#556547) was added to 100ul of cell suspension and incubated for 10min on ice. Cells were then washed and stained with 5ul of Propidium iodide (Invitrogen#00-6990) prior to flow cytometry. AM ($CD45^+$Siglec F^+ $CD11c^+$) populations that were either $CD11b^+$ or$Cd11b^-$ were gated and $Annexin^+$ cells were plotted against propidium iodide.

Analysis of NOX2 NADPH oxidase expression and activity in neutrophils, macrophages and monocytes

Nonadherent bone marrow neutrophils, peritoneal or alveolar macrophages were isolated as described.[2,4,7] Bone marrow monocytes were isolated with an EasySep Mouse Monocyte Isolation Kit (STEMCELL Technologies, Vancouver, BC, Canada). To isolate peripheral blood mononuclear cells, 2-3mL whole mouse blood was layered over Histopaque 1077, spun at 400Xg for 30 minutes at room temperature and the interface harvested, and washed two times in PBS containing 2mM EDTA and 2% FBS.

Neutrophil NOX2 activity was monitored by flow cytometry using dihydrorhodamine 123 (DHR) on peripheral blood samples or cytochrome C reduction with phorbol 12-myristate 13-acetate (PMA) stimulation of bone marrow neutrophils.[2,8]Peripheral blood mononuclear cells were surface stained with Ly6C, CD115 and CD11b (Table 1), stimulated with PMA in the presence of DHR, and NOX2 activity analyzed by flow cytometry for DHR fluorescence in $Ly6C^+CD115^+Cdllb^+$ peripheral blood monocytes. The stimulation index of $Ly6C^+CD115^+Cd11b^+$ peripheral blood monocytes was calculated as the mean fluorescence of PMA-stimulated cells divided by the mean fluorescence of the unstimulated cells.[9] The nitroblue tetrazolium (NBT) assay to detect superoxide as formazan deposition following NBT oxidation was used to assay macrophage NOX2 activity.[7,10] Briefly, $0.125X10^6$ resident alveolar or peritoneal macrophages were plated on 8-well permanox slides (Thermo Fisher Scientific) in RPMI containing 20% FBS, 1% pen-step solution, 1% L-glutamine, and 1% non-essential amino acids, and allowed to adhere overnight at 37°C. The next day, wells were washed once with PBS and incubated at 37°C for ten minutes in RPMI saturated with NBT. Serum opsonized zymosan was added at a final concentration of 0.025mg/mL, spun onto cells and incubated at 37°C for an additional fifteen minutes. After washing, air-dried slides were fixed in methanol and counter stained with 0.1% Safranin O. Macrophages containing phagocytized particles were counted, 200 per sample, with NBT-positive cells scored by the presence of formazan in phagosomes.

Cell lysates of bone marrow neutrophils, bone marrow monocytes or peritoneal macrophages were prepared and processed for Western blots as described.[2,7] Blots were probed with antibodies to detect mouse $p67^{phox}$ (Abcam, Cambridge, MA, USA) and β-actin (Cell Signaling Technologies, Danvers, MA, USA). Signals were detected with ECL (Thermo Fisher

Scientific, Berkeley, CA, USA) and visualized in a GelDoc Go System (Bio-Rad Laboratories, Hercules, CA, USA), and quantified with ImageJ (NIH, Bethesda, MD, USA).

Analysis of sorted resident alveolar macrophages by RNA-seq

BAL alveolar macrophages were studied from 4 week and 12 week old control and *Cybb*^{KO} mice. For each replicate, BAL AM from various groups of mice were sorted into RPMI+20%FBS on the basis of CD45^{+}Ly6G^{-}SiglecF^{+}CD11c^{+} markers and CD11b expression (CD11b^{+}or CD11b). To achieve a sufficient number of AM cells (~50,000) per each replicate sample, 2 to 3 mice from same group were pooled. Cells were centrifuged followed by resuspension in RLT-plus RNA Lysis buffer (Qiagen). RNA isolation was done using RNAeasy micro-plus columns (Qiagen). 3 independent replicates from each group were analyzed. RNA seq libraries were generated with Clontech SMARTer kits and sequencing were performed on a HiSeq3000 sequencer.[11]

RNA-seq reads were aligned to the mouse genome (Ensembl release 76 primary assembly) with STAR version 2.4.0b.[12] Gene counts were derived from the number of uniquely aligned unambiguous reads by Subread:featureCount version 1.5.3.[13] All gene counts were then imported into the R/Bioconductor package EdgeR[14] and TMM normalization size factors were calculated to adjust for samples for differences in library size. The TMM size factors and the matrix of counts were then imported into the R/Bioconductor package Limma.[15] Linear modeling (limma/voom) was used to compare gene expression across samples. The differential expression results were filtered for only those genes with Benjamini-Hochberg false-discovery rate adjusted p-values less than or equal to 0.05. Heatmaps, Volcano plots and Venn diagrams were created using R. Hallmark gene sets[16] were analyzed using applicable gene set enrichment (GSEA) method.[17,18]

Analysis of resident peritoneal macrophage gene expression by microarray

Peritoneal leukocytes were obtained by lavaging peritoneal cavities of WT and X-CGD with PBS+2mM EDTA. Tissue resident macrophages (B220^{-}, CD115^{+}, F4/80^{hi}, MHC class II^{-} and B220^{-}, CD115^{+}, F4/80^{lo}, MHC class II^{hi}) were sorted directly into RLT buffer and RNA extracted using RNA-easy Micro kit (Qiagen). For microarrays, RNA transcripts were amplified and cDNAs prepared using the WTA2 kit (Sigma Aldrich) according to manufacturer's protocol. cDNAs were labeled using Kreatech Cy5 labeling kits and hybridized onto Agilent Mouse v2

4x44k microarrays (G4846A-026655) as per manufacturer's protocol. Slides were scanned on an Agilent C-class Microarray scanner and gridding and image analysis performed using Feature Extraction (v11.5.1.1, Agilent Technologies). Spot intensity data was processed using Partek Genomics Suite software and significance analysis done using Linear Models for Microarrays (limma).[15] Adjusted p-values were calculated by the Benjamini and Hochberg false discovery rate.[19] Gene set enrichment analysis was performed for Hallmark pathways using GSEA (http://www.broad.mit.edu/gsea).[18]

ATAC-Seq

For ATAC-Seq analysis, BAL AM were sorted from various groups of mice into RPMI+20%FBS on the basis of $CD45^+LY6G^-$Siglec F^+CD11c^+ markers and CD11b expression ($CD11b^+$or $CD11b^-$). Two to 3 mice from each group were pooled to achieve 50,000 AM for each replicate and at least 3 independent replicates for each group were analyzed. Cells were processed and libraries generated using the method described by Corces et al.[20] Libraries were amplified using barcode primers (Table 3), as described.[21] After library amplification, fragments were size-selected with SPRI beads (Beckman Coulter) with ratios of 0.9X and 1.8X for right and left sided selection.[11] Sequencing was performed using a HiSeq 2500 sequencer. Peaks were generated with MACS2 using the ATAC-seq processing pipeline developed by the Kundaje lab (http://github.com/kundajelab/atac_dnase_pipeline version 0.3.3).[22] Consistency among replicates was assessed based on irreproducible Discovery Rates.[23] Differential Binding peaks were identified with R package DiffBind. Signal tracks were visualized with in WashU Epigenome browser.[24] Transcription factor motif analysis was performed with Homer.[25] After identifying peaks with significant ATAC-seq signal changes using DiffBind, genes that have any such peaks within 500kb of the transcription starting sites (TSS) were identified. Enrichment of these genes in the Hallmark gene sets were tested using the hypergeometric test. Gene sets showing significant enrichment were determined by FDR<=0.05.

We also adopted CHIP seq data from Lavin et al 2014(GSM1545980, GSM1545981, GSM1545979, GSM1545979, GSM1562259)[26] for some of our analysis. ChIP seq reads were first retrieved from GEO (GSE63341), and mapped to the mm10 genome. Peaks were identified and ChIP-seq coverage tracks were generated with MACS2 using the AQUAS TF and histone ChIP-seq pipeline with the "histone" option (https://github.com/kundajelab/chipseq_pipeline, version 0.3.3).[22]

In vitro stimulation of resident alveolar and peritoneal macrophages

Resident alveolar and peritoneal macrophages were isolated from naïve wild type C57BL/6J, Ncf2$^{fl/fl}$, *Ncf2*^{KO}, or Ncf2^{LysMcre} mice for in vitro stimulation studies. To harvest AM, BAL was collected from 8-10 sequential lavages and cells washed with RPMI +20%FBS. To harvest RPM, peritoneal lavage was collected from 2 sequential lavages of 8ml each and washed with RPMI +20%FBS. In both cases, washed cells were resuspended in 500ul of the same culture media, counted, and 70,000 cells were plated in individual wells of 96 well tissue culture plates with RPMI +20% FBS. After 2 hrs of incubation at 2 hrs at 37°C with 5% CO2, non-adherent cells were aspirated and remaining cells were washed and used for stimulation experiments.

To study responses to either TLR4 or TLR2 agonists, the adhered cells treated with either UltraPure LPS (Invivogen, from E coli) at a dose of 10ng/ml, or Pam3csk4 (Invivogen) at a dose of 100ng/ml, in addition to an unstimulated control group incubated in only RPMI +20% FBS. After 4 hrs of treatment, RNA was prepared from the cells using Qiagen RNAeasy plus RNA isolation kit followed by RT-qPCR.

Zymosan induced inflammation

For zymosan-induced lung inflammation, mice were challenged with zymosan (isolated from *Saccharomyces cerevisiae)* (Sigma) intra-nasally (IN) at a dose of 1ug/g as described.[4] After 18hrs, mice were euthanized and BAL analyzed for leukocyte counts and differential as described.[4] To study the lung response to remote tissue inflammation, sterile peritoneal inflammation was induced by intraperitoneal (i.p) injection of zymosan (Sigma) at a dose of 0.05mg/g (≈10-fold less than used in a systemic inflammatory response syndrome model.[27,28] At 48 hrs mice were euthanized and peritoneal cells were harvested by two sequential lavages with 8ml of ice-cold PBS with 2mM EDTA and 2%FBS. Peritoneal leukocyte counts were performed using a hemocytometer and the leukocyte differential was determined using Wright-Giemsa stained cytospins.[8] To examine the associated systemic effects of inflammation on the lung, BAL was analyzed for cell counts, differential, and ELISA. Lungs were inflated with 10% formalin and used for histologic evaluation following hematoxylin and eosin or diaminobenzidine staining for myeloperoxidase.[4]

References

1. Farley FW, Soriano P, Steffen LS, Dymecki SM. Widespread recombinase expression using FLPeR (flipper) mice. *Genesis*. 2000;28(3-4):106-110.
2. Jacob CO, Yu N, Yoo DG, et al. Haploinsufficiency of nadph oxidase subunit neutrophil cytosolic factor 2 is sufficient to accelerate full-blown lupus in nzm 2328 mice. *Arthritis Rheumatol* 2017;69(8):1647-1660.
3. Clausen BE, Burkhardt C, Reith W, Renkawitz R, Förster I. Conditional gene targeting in macrophages and granulocytes using LysMcre mice. *Transgenic Res*. 1999;8(4):265-277.
4. Song Z, Huang G, Chiquetto Paracatu L, et al. NADPH oxidase controls pulmonary neutrophil infiltration in the response to fungal cell walls by limiting LTB4. *Blood*. 2020;135(12):891-903.
5. Brody SL, Gunsten SP, Luehmann HP, et al. Chemokine receptor 2-targeted molecular imaging in pulmonary fibrosis. 2020.
6. Deady LE, Todd EM, Davis CG, et al. L-Plastin Is Essential for Alveolar Macrophage Production and Control of Pulmonary Pneumococcal Infection. *Infection and Immunity*. 2014;82(5):1982-1993.
7. Bagaitkar J, Huang J, Zeng MY, et al. NADPH oxidase activation regulates apoptotic neutrophil clearance by murine macrophages. *Blood*. 2018;131(21):2367-2378.
8. Bagaitkar J, Pech NK, Ivanov S, et al. NADPH oxidase controls neutrophilic response to sterile inflammation in mice by regulating the IL-1alpha/G-CSF axis. *Blood*. 2015;126(25):2724-2733.
9. Vowells SJ, Fleisher TA, Sekhsaria S, Alling DW, Maguire TE, Malech HL. Genotype-dependent variability in flow cytometric evaluation of reduced nicotinamide adenine dinucleotide phosphate oxidase function in patients with chronic granulomatous disease. *J Pediatr*. 1996;128(1):104-107.
10. Huang J, Canadien V, Lam GY, et al. Activation of antibacterial autophagy by NADPH oxidases. *Proc Natl Acad Sci U S A*. 2009;106(15):6226-6231.
11. Li YN, Kong WJ, Yang W, et al. Single-Cell Analysis of Neonatal HSC Ontogeny Reveals Gradual and Uncoordinated Transcriptional Reprogramming that Begins before Birth. *Cell Stem Cell*. 2020;27(5):732-+.
12. Dobin A, Davis CA, Schlesinger F, et al. STAR: ultrafast universal RNA-seq aligner. *Bioinformatics*. 2013;29(1):15-21.
13. Liao Y, Smyth GK, Shi W. featureCounts: an efficient general purpose program for assigning sequence reads to genomic features. *Bioinformatics*. 2014;30(7):923-930.
14. Robinson MD, McCarthy DJ, Smyth GK. edgeR: a Bioconductor package for differential expression analysis of digital gene expression data. *Bioinformatics*. 2010;26(1):139-140.

15. Ritchie ME, Phipson B, Wu D, et al. limma powers differential expression analyses for RNA-sequencing and microarray studies. *J Nucleic acids research*. 2015;43(7):e47-e47.

16. Liberzon A, Birger C, Thorvaldsdottir H, Ghandi M, Mesirov JP, Tamayo P. The Molecular Signatures Database (MSigDB) hallmark gene set collection. *Cell Syst*. 2015;1(6):417-425.

17. Mootha VK, Lindgren CM, Eriksson KF, et al. PGC-1alpha-responsive genes involved in oxidative phosphorylation are coordinately downregulated in human diabetes. *Nat Genet*. 2003;34(3):267-273.

18. Subramanian A, Tamayo P, Mootha VK, et al. Gene set enrichment analysis: a knowledge-based approach for interpreting genome-wide expression profiles. *Proc Natl Acad Sci U S A*. 2005;102(43):15545-15550.

19. Benjamini YH, Yosef. Controlling The False Discovery Rate - A Practical And Powerful Approach To Multiple Testing. *J Royal Statist Soc*. 1995;Series B(57):289 - 300.

20. Corces MR, Trevino AE, Hamilton EG, et al. An improved ATAC-seq protocol reduces background and enables interrogation of frozen tissues. *Nat Methods*. 2017;14(10):959-962.

21. Buenrostro JD, Giresi PG, Zaba LC, Chang HY, Greenleaf WJ. Transposition of native chromatin for fast and sensitive epigenomic profiling of open chromatin, DNA-binding proteins and nucleosome position. *Nat Methods*. 2013;10(12):1213-1218.

22. Roadmap Epigenomics C, Kundaje A, Meuleman W, et al. Integrative analysis of 111 reference human epigenomes. *Nature*. 2015;518(7539):317-330.

23. Li QH, Brown JB, Huang HY, Bickel PJ. Measuring Reproducibility of High-Throughput Experiments. *Annals of Applied Statistics*. 2011;5(3):1752-1779.

24. Li D, Hsu S, Purushotham D, Sears RL, Wang T. WashU Epigenome Browser update 2019. *Nucleic Acids Res*. 2019;47(W1):W158-w165.

25. Heinz S, Benner C, Spann N, et al. Simple combinations of lineage-determining transcription factors prime cis-regulatory elements required for macrophage and B cell identities. *Mol Cell*. 2010;38(4):576-589.

26. Lavin Y, Winter D, Blecher-Gonen R, et al. Tissue-resident macrophage enhancer landscapes are shaped by the local microenvironment. *Cell*. 2014;159(6):1312-1326.

27. Whitmore LC, Hilkin BM, Goss KL, et al. NOX2 protects against prolonged inflammation, lung injury, and mortality following systemic insults. *J Innate Immun*. 2013;5(6):565-580.

28. Whitmore LC, Goss KL, Newell EA, Hilkin BM, Hook JS, Moreland JG. NOX2 protects against progressive lung injury and multiple organ dysfunction syndrome. *Am J Physiol Lung Cell Mol Physiol*. 2014;307(1):L71-82.

Table 1. Antibodies used for flow cytometry

Anti-mouse antibody	Clone	Company
B220	RA3-6B2	BD Pharmingen
CD45	30-F11	BD Horizon
CD3	145-2C11	BD Pharmingen
CD11b	M1/70	eBioscience
CD11c	HL3	BD Pharmingen
CD115	AFS98	eBioscience
CD64	X54-5/7.1	Biolegend
YM1	EPR15263	Abcam
Siglec F	E50-2440	BD Pharmingen
CD206	C068C2	Biolegend
MHCII	M5/114.15.2	BD Bioscience
LY6g	1A8	BD Horizon
LY6C	HK1.4	Biolegend
CCR2	SA203G11	Biolegend
Secondary	Ab150077	Abcam

Table 2. Antibodies used for CyTOF

Metal label	Specificity	clone	Company	Titration
89Y	CD45	30-F11	Fluidigm	0.25
141Pr	Ly6G/C (Gr1)	RB6-8C5	Fluidigm	0.25
142Nd	CD11c	N418	Fluidigm	0.25
144Nd	CD16/32	93	Fluidigm	0.5
145Nd	CD69	H1.2F3	Fluidigm	0.25
147Sm	CD36	No.72-1	Fluidigm	1
148Nd	CD11b(Mac1)	M1/70	Fluidigm	0.25
149Sm	CD19	6D5	Fluidigm	0.25
150Nd	Ly6c	HK1.4	Fluidigm	0.25
151Eu	CD64	x54-5/7.1	Fluidigm	1
152Sm	CD3e	145-2c11	Fluidigm	1
153Eu	CD274(PD-L1)	10F.9G2	Fluidigm	0.1
154Sm	Ter-119	TER119	Fluidigm	0.25
155Gd	SiglecF	E50-2440	BD Pharmingen	0.5
156Gd	CD14	Sa142	Fluidigm	0.25
159Tb	F4/80	BM8	Fluidigm	0.5
160Gd	CD62L	MEL-14	Fluidigm	0.25
161Dy	CD40	HM40-3	Fluidigm	1
162Dy	CD1d	1B1	Fluidigm	0.1
164Dy	CX3CR1	8F1/CXCR1	Fluidigm	0.25
165Ho	CD31(PECAM-1)	390	Fluidigm	0.5
166Er	CD326(EpCAM)	G8.8	Fluidigm	0.5
168Er	CD8a	53-6/7	Fluidigm	0.25
169Tm	CD206	C068C2	Fluidigm	0.5
170Er	NK1.1	PK136	Fluidigm	0.5
171Yb	CD44	IM7	Fluidigm	0.25
172Yb	CD4	RM4-5	Fluidigm	0.25
174Yb	MHC II (1A/1E)	M5/114.15.2	Fluidigm	0.5
176Yb	B220/CD45R	RA3-6B2	Fluidigm	0.5

Table 3. PCR TaqMan Primers (Thermo Fisher Scientific)

Genes	Primer details
Ccl2	Mm00441242_m1
Ccl3	Mm00441258_m1
Ccl4	Mm00443112_m1
Itgam(CD11b)	Mm00434455_m1
Chi3l3	Mm04213363_u1
Cxcl2	Mm00436450_m1
Gapdh	Mm99999915_g1
IL1a	Mm00439620_m1
IL1b	Mm00434228_m1
IL6	Mm00446190_m1
Isg15	Mm1705338_s1
MX1	Mm00487796_m1

Table 4. ATAC-Seq Primers

Sample name	Species	Primer number	Index
A	Mouse	1	TAAGGCGA
B	Mouse	2	CGTACTAG
C	Mouse	3	AGGCAGAA
D	Mouse	4	TCCTGAGC
E	Mouse	5	GGACTCCT
F	Mouse	6	TAGGCATG
G	Mouse	7	CTCTCTAC
H	Mouse	8	CAGAGAGG
I	Mouse	9	GCTACGCT
J	Mouse	10	CGAGGCTG
K	Mouse	11	AAGAGGCA
M	Mouse	12	GTAGAGGA
N	Mouse	13	GTCGTGAT
O	Mouse	14	ACCACTGT
P	Mouse	15	TGGATCTG

SUPPLEMENTAL FIGURE 1

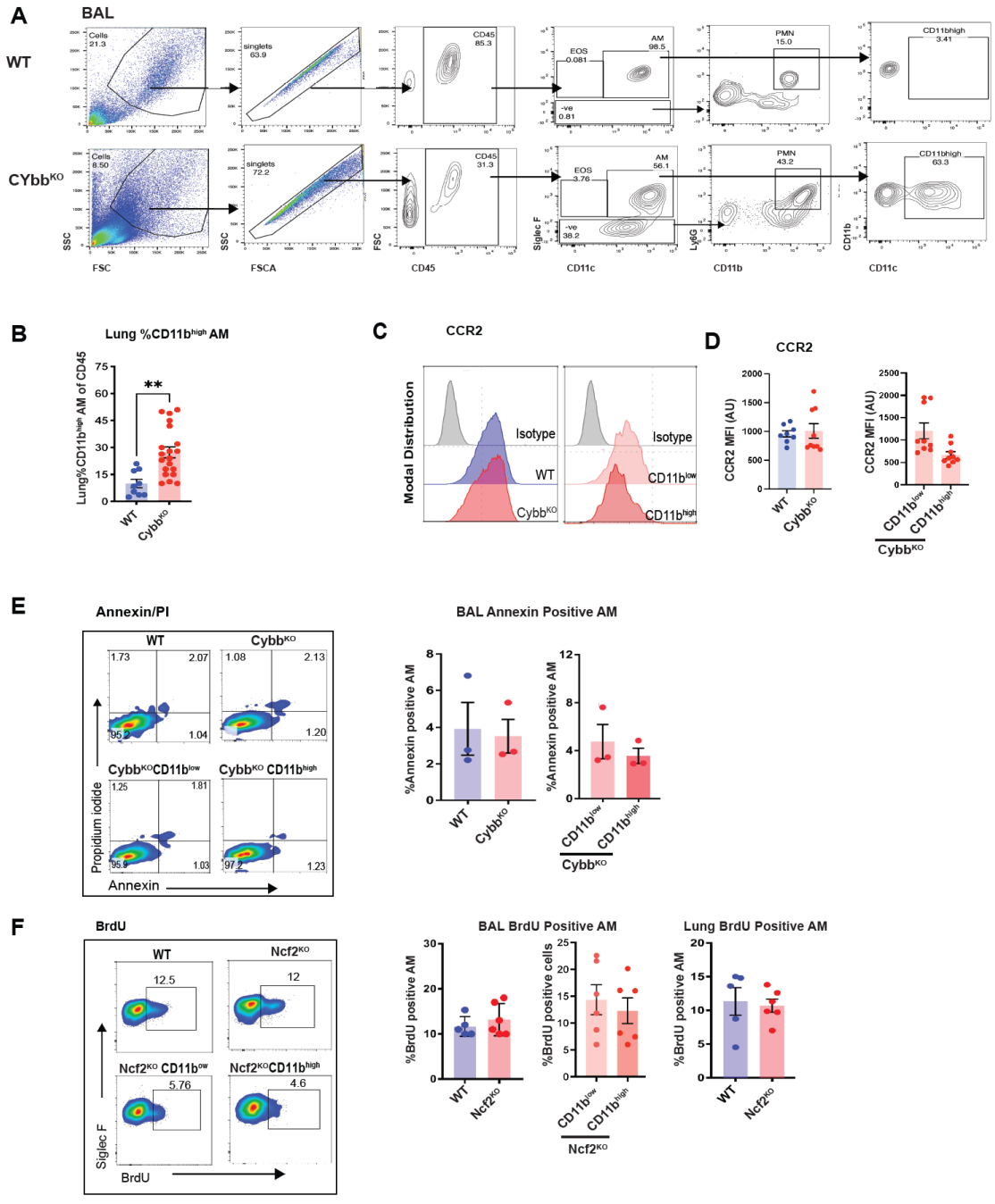

Supplemental Figure 1. Analysis of lung macrophages in mice with global deletion of NOX2.

A) Gating strategy for BAL flow cytometry. **B)** Flow cytometric analysis of CD11b^{high} AM in single cell suspensions prepared from lung tissue of 12-week-old WT and *Cybb*^{KO} mice. n≥5 for each group. **C)** Analysis of CCR2 expression by flow cytometry among different groups of AMs

from 12-week-old WT and *Cybb*^{KO} mice. **D)** CCR2 MFI in various groups of AMs from 12-week-old WT and *Cybb*^{KO} mice. n≥8 for each group. **E)** Flow cytometric analysis of BAL from 12-week-old mice for annexin-positive AM in WT vs *Cybb*^{KO} mice, as well as its quantification. n=3 in each group. **F)** Flow cytometric analysis for BrdU positive AM from 12-week-old WT and *Ncf2*^{KO} mice and its quantification in both BAL and lung tissues. n≥5 in each group. Bar graph data represented as mean ± SEM; Data represented for at least 2 set of experiments. Student 't' test was performed and *P< 0.05 **P<0.01, ***P<0.001 was considered as significant.

SUPPLEMENTAL FIGURE 2

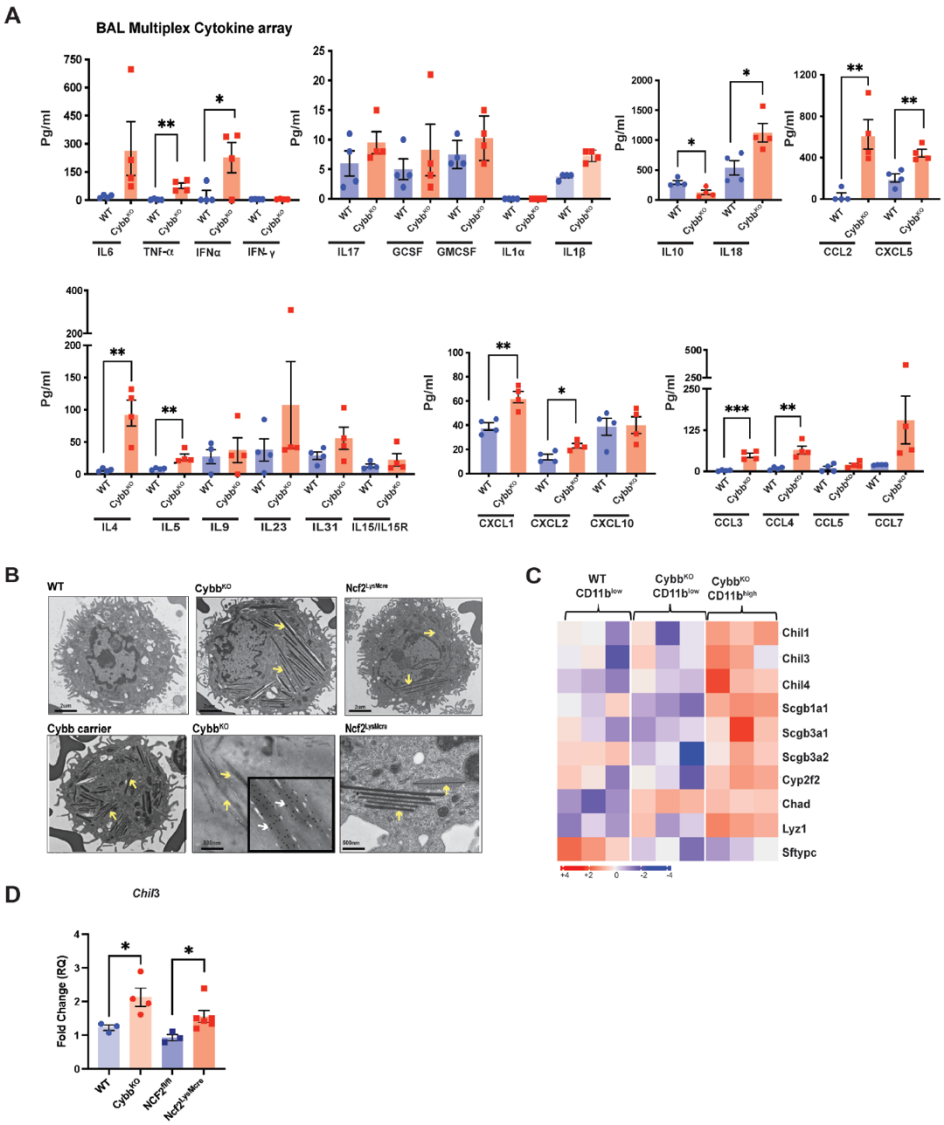

Supplemental Figure 2. Analysis of BAL cytokines and lung macrophages in NOX2-deleted mice.

A) Multiplex cytokine analysis of BAL WT and *Cybb*^{KO} mice at 12-weeks of age. n=4 for each group. **B)** TEM Images from WT, *Cybb*^{KO}, *Ncf2*$^{fl/fl}$ and *Ncf2*^{LysMCre} and *Cybb* carrier AM. Yellow arrows indicate membrane-bound YM1 crystals and white arrows indicate immunolabeling within the crystals with YM1 primary antibody. Representative image from samples from at least 2 different mice of each genotype. **C)** Heatmaps from RNAseq data from indicated groups of AM showing relative expression of genes for different chitinase like proteins (CLP) along genes for related secretory proteins. **D)** *Chil*3 expression by RT-qPCR in AM isolated from BAL samples of indicated groups of mice.

Bar graph data represented as mean ± SEM. Student 't' test was performed and *P< 0.05 **P<0.01, ***P<0.001 was considered as significant. *P< 0.05 **P<0.01, ***P<0.001 was considered as significant. n=4.

SUPPLEMENTAL FIGURE 3

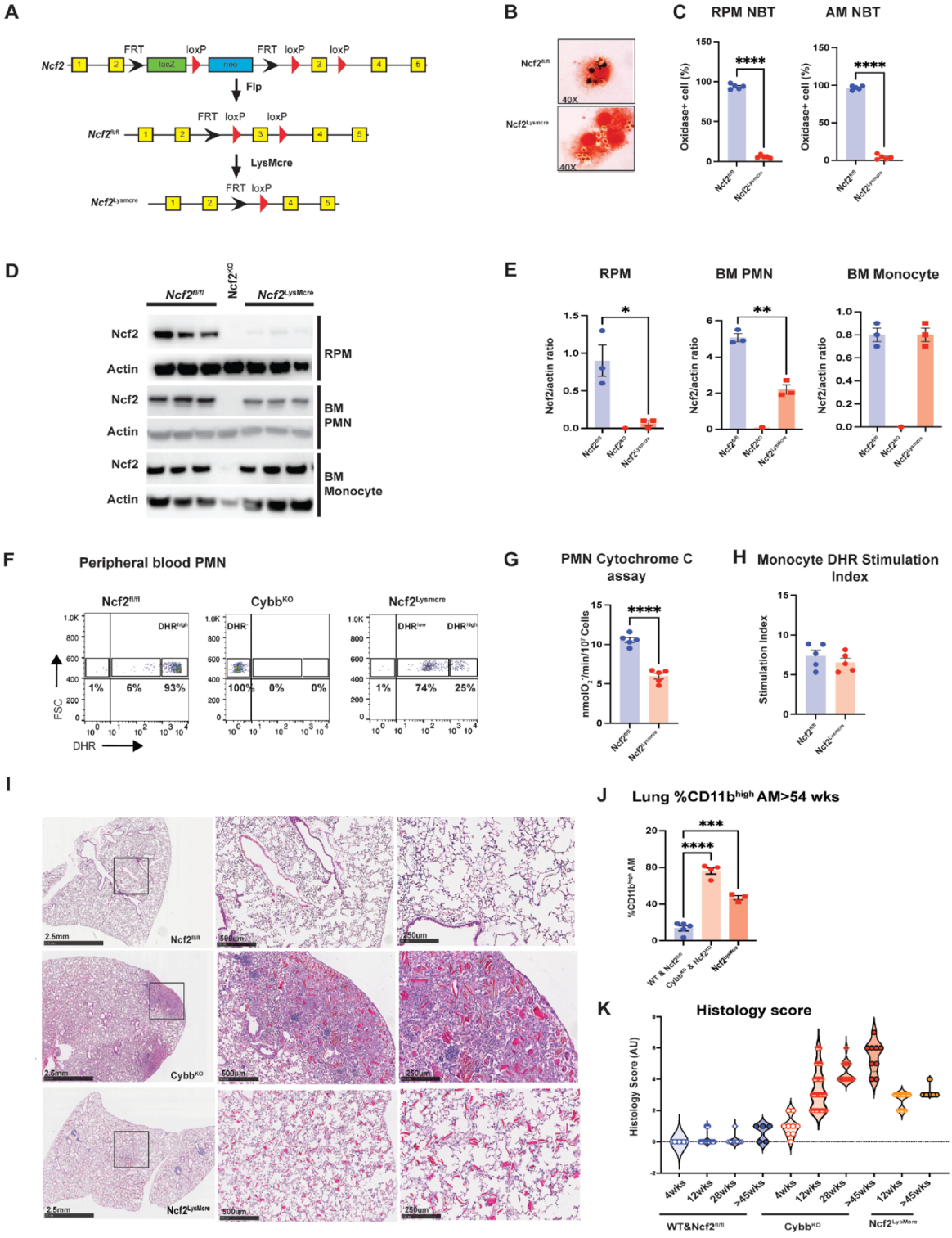

Supplemental Figure 3. Generation of *Ncf2*^{LysMcre} mice and comparative analysis of alveolar macrophages and lung histology in WT and *Cybb*^{KO} mice of different ages.
A) Schematic representation of the *Ncf2*$^{tm1a(EUCOMM)Wtsi}$ allele, the *Ncf2*$^{fl/fl}$ allele generated after Flp- mediated excision of the region between the 5' and 3' FRT sites, and the exon 3-deleted allele, *Ncf2*^{LysMcre}, after LysMCre-mediated excision between the 5' and 3' loxP sites. **B)** Nitroblue tetrazolium (NBT) assay for NOX2 activity in resident peritoneal macrophages (RPM) ingesting zymosan, showing NBT-positive phagosomes (purple) in *Ncf2*$^{fl/fl}$ RPM from *Ncf2*$^{fl/fl}$ and NBT-negative phagosomes in *Ncf2*^{LysMcre} RPM. **C)** Percent of oxidase positive (NBT positive) RPM and AM in *Ncf2*$^{fl/fl}$ and *Ncf2*^{LysMcre} mice. 200 cells scored per mouse. **D)** Western blots showing expression of NCF2 in RPM, bone marrow neutrophils (BM PMN) and bone marrow monocytes. Actin was used as a loading control, and representative blot is shown. **E)** Quantification of NCF2 levels in RPM, BM PMN and BM monocytes corresponding to (d), as assessed by ImageJ. **F)** Dihyrorhodamine (DHR) assay for NOX2 activity in peripheral blood PMN. Percent of DHR-high, low DHR-low and DHR-negative cells as indicated in Ncf2$^{fl/fl}$, Cybb^{KO} and Ncf2^{LysMcre} mice. Representative samples are shown. **G)** Superoxide production by cytochrome C assay of BM PMN from Ncf2$^{fl/fl}$ and Ncf2^{LysMcre} mice. **H)** Monocyte stimulation index calculated from DHR+ bone marrow monocytes in *Ncf2*$^{fl/fl}$ and *Ncf2*^{LysMcre} mice. Each data point represents one mouse. **I)** Hematoxylin-eosin staining of lung tissue from *Ncf2*$^{fl/fl}$, *Cybb*^{KO} and *Ncf2*^{LysMcre} mice aged 54 weeks or older. Representative data from ≥5 mice in each genotype. **J)** Percentage of lung CD11b^{high} cells in CD45^{+} Siglec F^{+} CD11c^{+} AM from older (>54 weeks) WT, *Ncf2*$^{fl/fl}$, *Cybb*^{KO} and *Ncf2*^{LysMcre} mice. **K)** Lung histology scores for WT and NOX2-deficient mice of different ages, using scoring system detailed in the Methods.
Bar graph data shown as mean ± SEM. Student's 't' test was performed for samples distributed in 2 groups and *P< 0.05 **P<0.01, ***P<0.001 were considered as significant. One-way ANOVA was done followed by Tukey's post hoc analysis comparing multiple groups. *P< 0.05 **P<0.01, ***P<0.001 were considered as significant. Data represented from at least 2 independent experiments.

SUPPLEMENTAL FIGURE 4

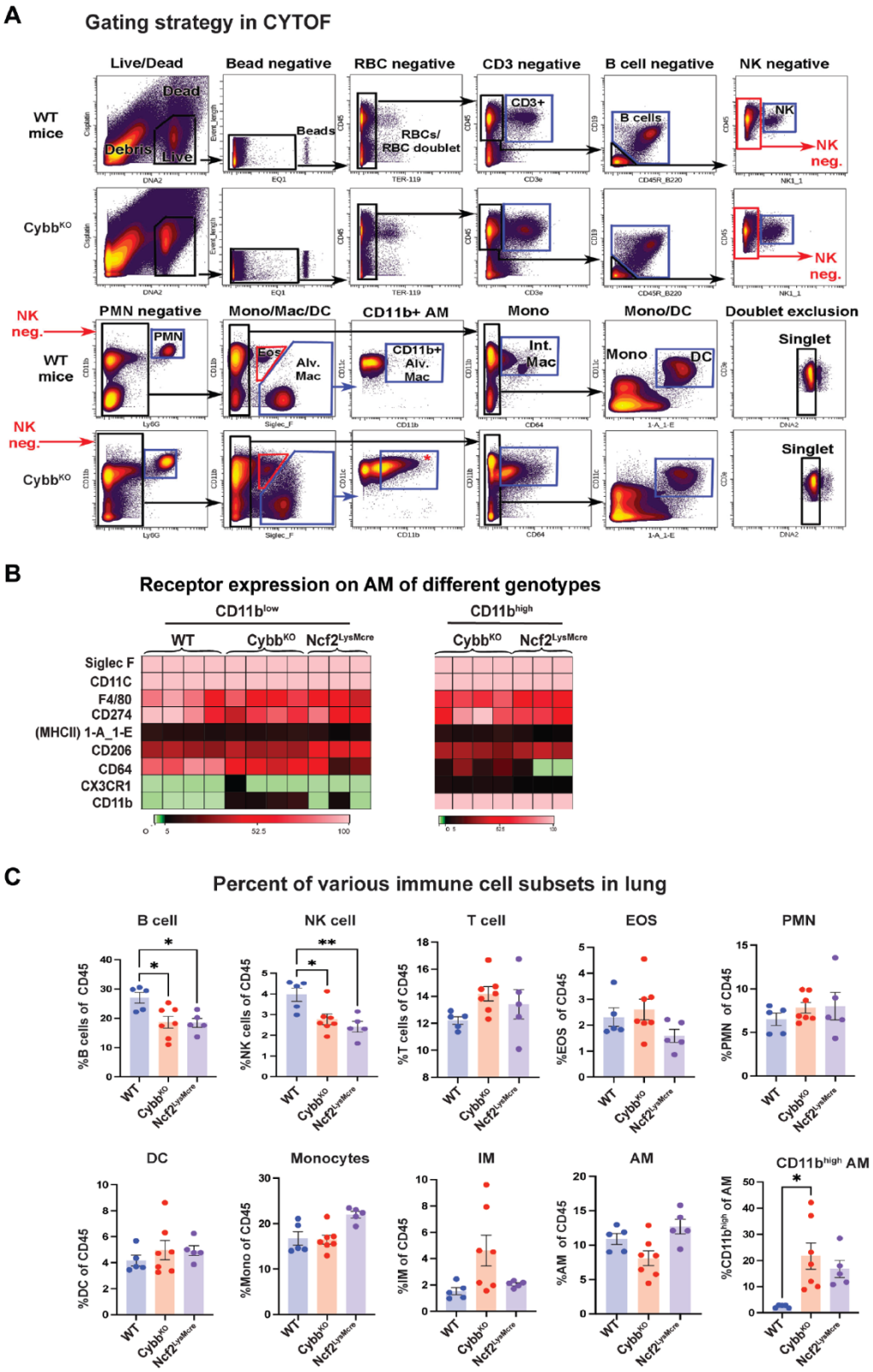

Supplemental Figure 4: CYTOF analysis of lung tissues from WT and NOX2-deleted mice.
A) Gating strategy of CyTOF for lung tissues from WT, *Cybb*^{KO}, *NCF2*$^{fl/fl}$ and *NCF2*^{LysMcre} mice. **B)** Heatmaps of median metal intensity of surface receptor staining showing the raw data for the indicated groups of alveolar macrophages from lung tissue. n≥3. **C)** Bar diagram showing different immune cell populations of lung tissues obtained from CyTOF data. n≥4. Bar graph data represented as mean ± SEM; One-way ANOVA was done comparing more than 3 groups followed by Tukey's post hoc analysis. $P < 0.05$ was considered as significant. Data represented for at least 2 set of experiments.

SUPPLEMENTAL FIGURE 5

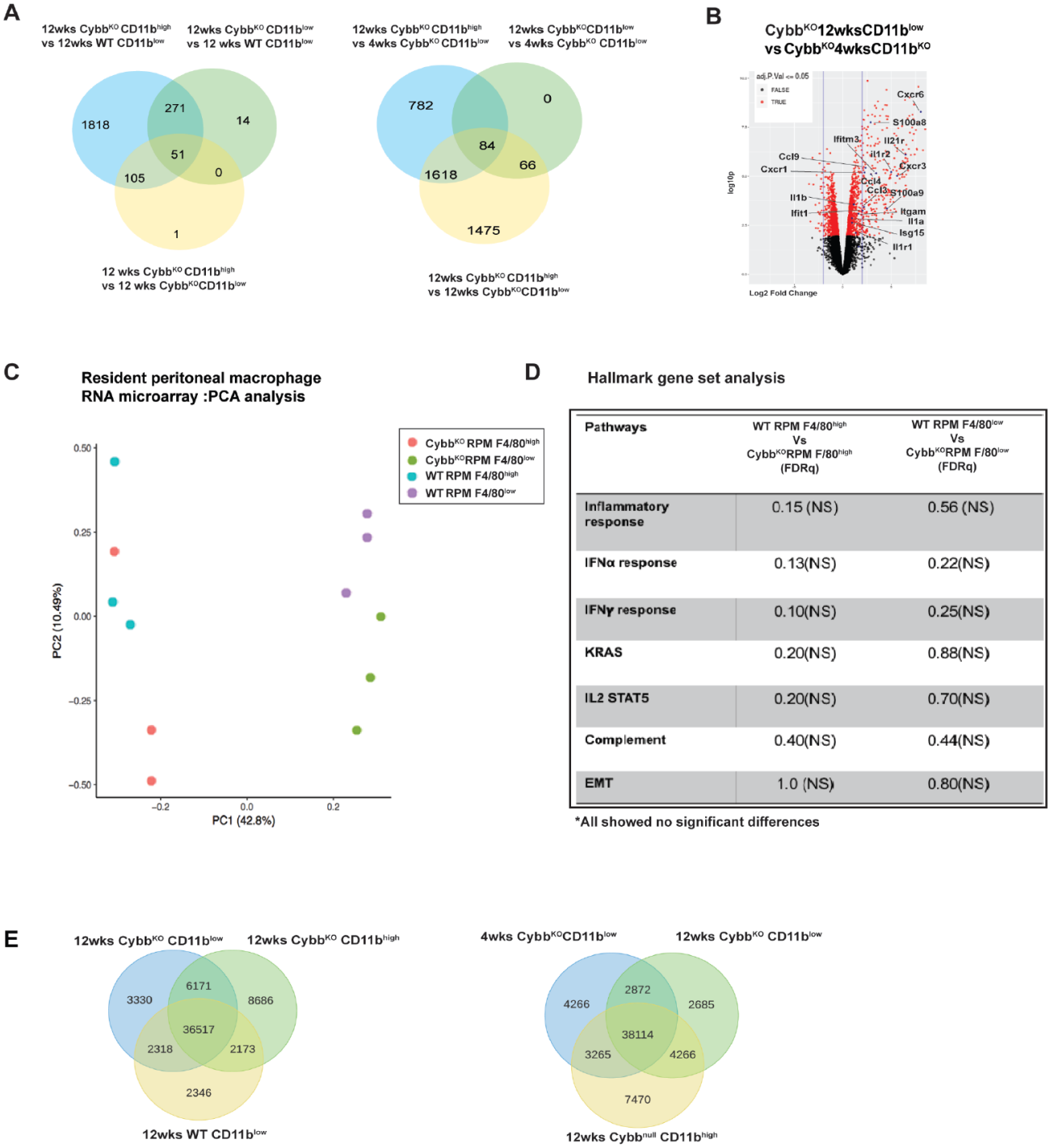

Pathways	WT RPM F4/80^high Vs Cybb^KO RPM F/80^high (FDRq)	WT RPM F4/80^low Vs Cybb^KO RPM F/80^low (FDRq)
Inflammatory response	0.15 (NS)	0.56 (NS)
IFNα response	0.13(NS)	0.22(NS)
IFNγ response	0.10(NS)	0.25(NS)
KRAS	0.20(NS)	0.88(NS)
IL2 STAT5	0.20(NS)	0.70(NS)
Complement	0.40(NS)	0.44(NS)
EMT	1.0 (NS)	0.80(NS)

*All showed no significant differences

Supplemental Figure 5. Transcriptional and epigenetic analysis of signatures in alveolar and peritoneal macrophages from mice with global deletion of NOX2.
A) Venn diagram of differences of gene expression among various groups showing the highest alterations of uniquely differentially expressed genes were found in *Cybb*^{KO} CD11b^{high} AM

compared to WT CD11b^{low} AM from 12-week-old mice. **B)** Volcano plot showing differentially expressed genes in CD11b^{low} AM from *Cybb*^{KO} mice at 12 weeks compared to 4 weeks of age. Some of the genes significantly upregulated at 12 weeks of age are indicated, selected from those in the Hallmark inflammatory response and/or interferon response gene sets**. C)** PCA analysis of microarray data showing variation of transcriptomes in the two resident peritoneal macrophage (RPM) populations (CD115+F4/80^{low} MHCII^{high} and CD115+F4/80^{high} MHCII^{low}) from 12-week-old WT and *Cybb*^{KO} mice. **D)** Hallmark gene set enrichment analysis between WT and *Cybb*^{KO} RPM had no significant differences, as shown in these examples. **E)** Venn diagram comparing the number of ATAC seq peaks among the various groups of alveolar macrophage samples sorted from 12-week-old WT and *Cybb*^{KO} mice.

SUPPLEMENTAL FIGURE 6

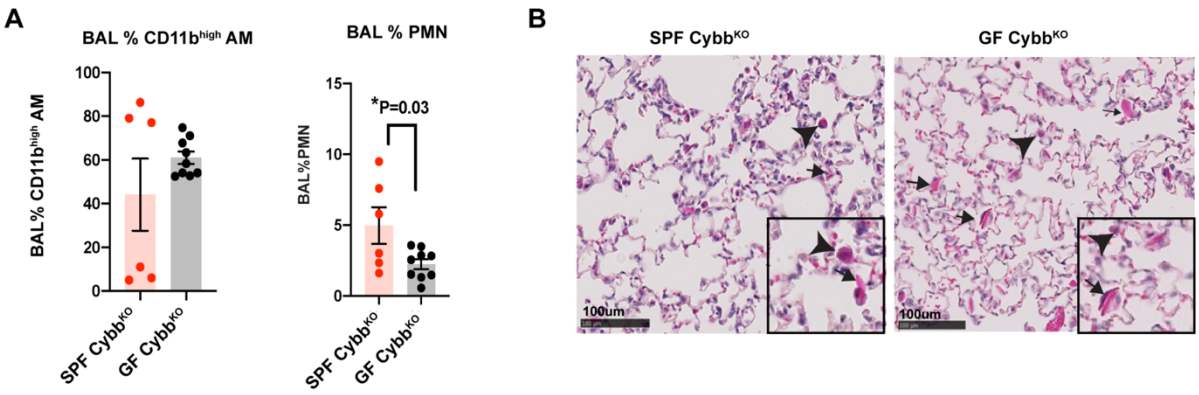

Supplemental Figure 6. Impact of microbiota on development of alveolar inflammation in mice with global deletion of NOX2.
A) Flow cytometric analysis of BAL from specific pathogen free (SPF) and germ free (GF) *Cybb*^{KO} mice, comparing % of CD11b^{high} AM and %PMN. Male mice n≥6 in each group.
B) Hematoxylin-eosin staining of lung tissue showing eosinophilic macrophages (arrowheads) and extracellular crystals (arrows) in germ free *Cybb*^{KO} mice and *Cybb*^{KO} SPF mice. Representative image from 6 samples of each group. Scale bar: 100um.
Student's 't' test was performed for samples distributed in 2 groups and *P< 0.05 **P<0.01, ***P<0.001 were considered as significant. Data represented from at least 2 independent experiments.

SUPPLEMENTAL FIGURE 7

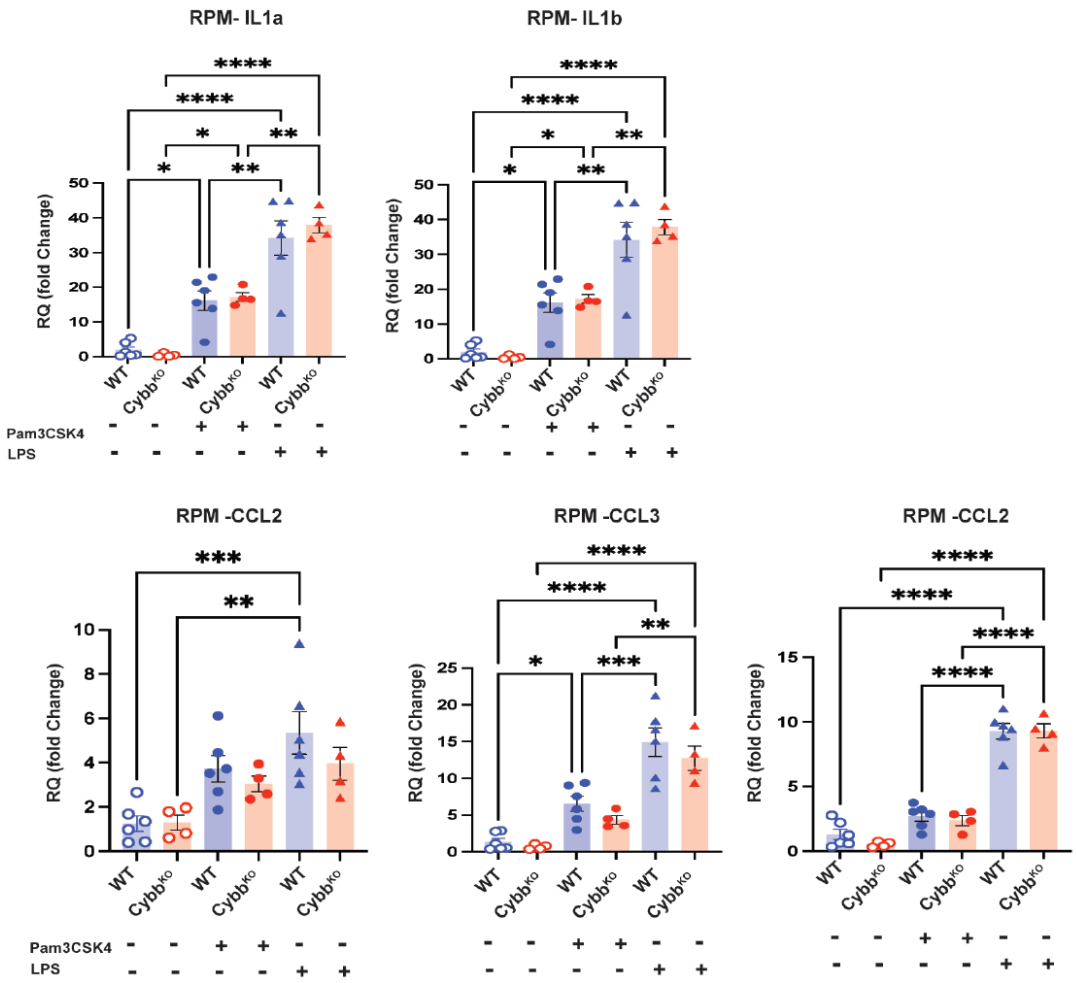

Supplementary Figure 7. TLR stimulated inflammatory gene expression in resident peritoneal macrophages.
Resident peritoneal macrophages were isolated from 12-week-old WT and *Cybb*^{KO} mice, stimulated with Pam3CSK4 (100ng/ml) or LPS (10ng/ml) for 4 hrs and proinflammatory genes assayed by qRT-PCR. Bar graph data shown as mean ± SEM. One-way ANOVA was done followed by Tukey's post hoc analysis comparing multiple groups. *P< 0.05 **P<0.01, ***P<0.001 were considered as significant. Data represented from at least 2 independent experiments.

SUPPLEMENTAL FIGURE 8

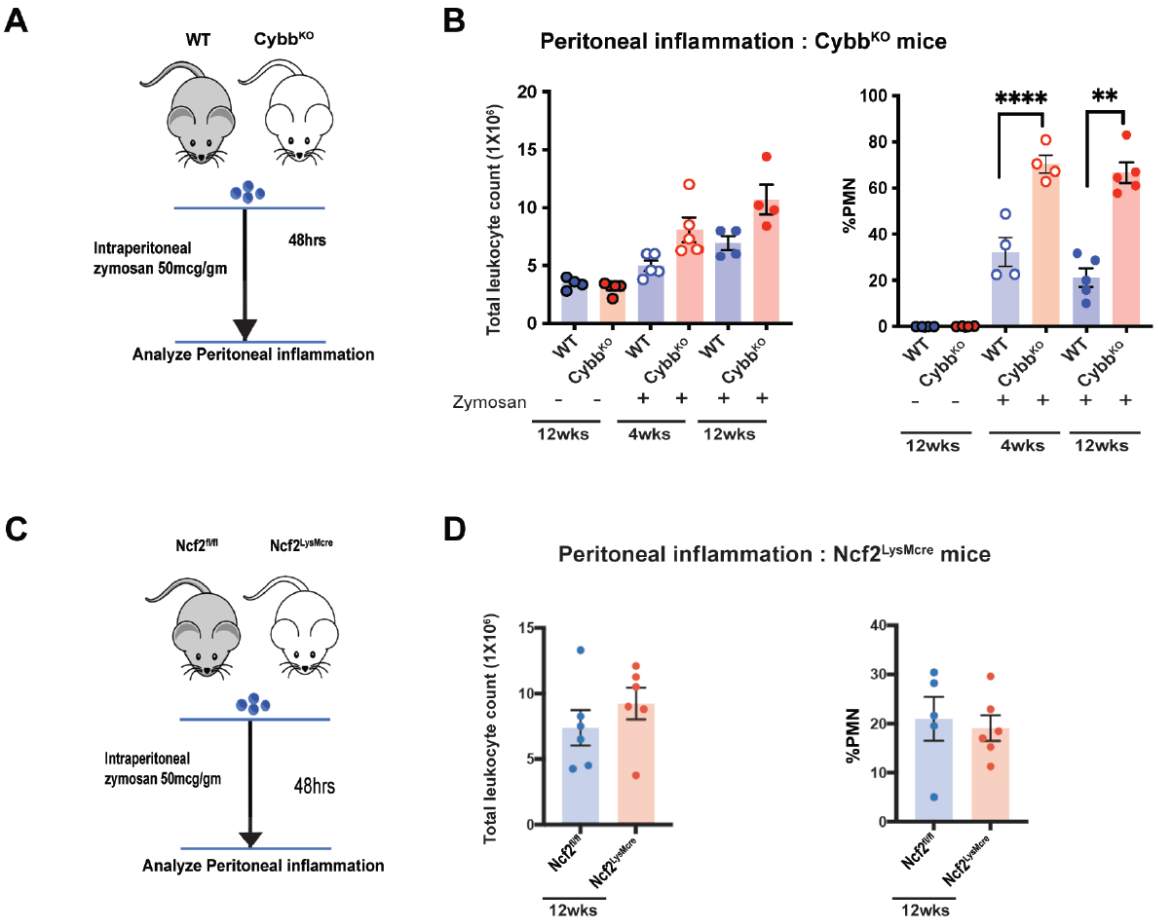

Supplemental Figure 8. Zymosan-induced peritonitis in NOX2-deleted mice.
A) Schema for zymosan-induced peritonitis in WT and *Cybb*^{KO} mice**. B)** Peritoneal cell counts and %PMN at 48hrs following IP instillation of zymosan in 4-week-old and 12-week-old WT and *Cybb*^{KO} mice. Data represented as mean ± SEM; n≥4. **C)** Schema for zymosan-induced peritonitis in *Ncf2*$^{fl/fl}$ and *Ncf2*^{LysMCre} mice**. D)** Peritoneal cell counts and %PMN at 48hrs following IP instillation of zymosan in 12-week-old *Ncf2*$^{fl/fl}$ and *Ncf2*^{LysMCre} mice. Data represented as mean ± SEM; n≥5. Student's 't' test was performed for samples distributed in 2 groups and *P< 0.05 **P<0.01, ***P<0.001 were considered as significant. Bar graph data represented for at least 2 set of experiments.